

André Dumont medallist lecture 2017

Routing of terrestrial organic matter from the Congo River to the ultimate sink in the abyss: a mass balance approach

FRANÇOIS BAUDIN¹, CHRISTOPHE RABOUILLE² & BERNARD DENNIELOU³¹ ITeP, SU & CNRS, Paris, France.² LSCE, CEA-CNRS-UVSQ & IPSL, Gif-sur-Yvette, France.³ IFREMER, Unité de Recherche Géosciences marines, Plouzané, France.

* corresponding author: francois.baudin@sorbonne-universite.fr.

ABSTRACT. We address the role of the Congo River sediment dispersal in exporting and trapping organic carbon into deep offshore sediments. Of particular interest is the Congo submarine canyon, which constitutes a permanent link between the terrestrial sediment sources and the marine sink. The Congo River delivers an annual sediment load of ~40 Tg (including 2 Tg of C) that feed a mud-rich turbidite system. Previous estimates of carbon storage capacity in the Congo turbidite system suggest that the terminal lobe complex accounts for ~12% of the surface area of the active turbidite system and accumulates ~18% of the annual input of terrestrial particulate organic carbon exiting the Congo River. In this paper, we extend the approach to the whole active turbidite depositional system by calculating an average burial of terrestrial organic matter in the different environments: canyon, channel, and levees. We estimate that between 33 and 69% of terrestrial carbon exported by the Congo River is ultimately trapped in the different parts of turbidite system and we evaluate their relative efficiency using a source to sink approach. Our carbon budget approach, which consider annual river discharge *versus* offshore centennial accumulation rates, indicates that about half of the total particulate organic matter delivered yearly by the Congo River watershed escapes the study area or is not correctly estimated by our deep offshore dataset and calculations.

KEYWORDS: recent sediments, Congo turbidite system, organic carbon, burial efficiency, source-to-sink.

1. Introduction

The riverine systems that extend from terrestrial drainage basins, across the continental margins, to the deep sea are major actors of the Earth's sedimentary cycle. They have also a fundamental role for the long-term carbon cycle regarding burial of terrestrial organic carbon in marine sediments (Schlünz & Schneider, 2000; Burdige, 2005; Galy et al., 2007; Hilton et al., 2008; Leithold et al., 2016) and hence for climate regulation. The annual global terrestrial organic matter burial is estimated between 40 and 60 Tg C with almost 75–85% deposited in the large-river deltas and the adjacent shelves (Bernier, 1989; Hedges & Keil, 1995; Burdige, 2005). Nevertheless, a significant fraction of terrestrial organic carbon entering the ocean bypasses shelves and is transferred to the deep sea through submarine canyons (Monaco et al., 1990; Canals et al., 2006; Heussner et al., 2006; Sanchez-Vidal et al., 2012). However, it is still not clear to what extent the fraction of terrestrial organic carbon carried over to the deep-sea basin is buried and trapped on geological timescales. The organic carbon routing in present-day riverine systems is studied from the areas of its production to the areas of its burial, through mass balances, in the so-called source to sink (S2S) approaches.

The efficiency of the transfer to the deep sea and subsequent trapping of terrestrial organic particles has been studied for small river systems with a direct connection to submarine canyons (Hsu et al., 2014; Kuehl et al., 2016). The studied rivers are usually related to mountainous environments along active margins (i.e., Taiwan, New Zealand) where these small systems are associated with large sedimentary fluxes and show a relatively high efficiency in storing terrestrial particulate organic matter (Hsu et al., 2014; Kuehl et al., 2016). By contrast, S2S approaches are less common for large drainage basins, with the exception of the Amazon River system (Leithold et al., 2016), which is a dispersal system with energetic shelves where sediment is extensively reworked and particulate organic matter undergoes intense biogeochemical remineralization (Blair & Aller, 2012).

In this work, we address the fate of terrestrial organic carbon exported into the deep sea by the second largest river in the world, the Congo River. Of particular interest is the Congo deep-sea channel and submarine canyon, which is connected to the river's estuary, and therefore constitutes a permanent link between the terrestrial sediment source and the deep-sea sink, resembling the small active rivers mentioned above. The Congo River delivers an annual sediment load of ~40 Tg that presently feed one of the largest mud-rich turbidite system in the world, with a surface reaching 21,400 km² for the active system and 300,000 km² for

the entire fan, including numerous abandoned turbidite systems. Therefore, it is important to understand the transport pathway and the accumulation efficiency of terrestrial organic carbon in such a setting and especially in the different parts of the active turbidite system.

Previous estimates of carbon storage capacity have been made on the terminal lobes (Rabouille et al., 2009, 2019; Stetten et al., 2015), a very active domain that accounts for only a limited proportion (~12%) of the surface area of the present-day active Congo turbidite system. In this paper, we extend the approach to the upstream active channel-levees and canyon using a multidisciplinary dataset including sediment traps to quantify the fate of sinking organic carbon, sedimentation rate estimates along the turbidite system, sediment characteristics and particularly its organic content. This allows calculating an average annual burial of terrestrial organic matter in the different compartments of the turbidite system. In our S2S approach, we estimate the proportion of terrestrial carbon trapped and the burial efficiency in these compartments by comparing the obtained organic burial fluxes to the annual discharge of the Congo River.

2. Background

2.1. Congo River

The Congo River drains the second largest watershed of the world (3.7 10⁶ km²) and concentrates about 38% of the yearly run-off from Africa (Laraque et al., 2001). The Congo basin has a humid tropical climate with a mean annual precipitation close to 1550 mm (Mahé, 1995) and a mean temperature over 20 °C. The main tributaries of the Congo River are the Kasai and Lomami Rivers on its southern side, and the Ubangui and the Likouala Rivers on its northern side (Fig. 1A). The hydrological regime of the Congo River at the Brazzaville/Kinshasa station (450 km upstream of its mouth) is typically equatorial with extremely limited fluctuations of the water discharge (Fig. 1B). Indeed, the Congo River shows probably the most homogenous hydrological regime on Earth with low interannual variations of the yearly discharges: 33,300–55,200 m³.s⁻¹ (41,000 m³.s⁻¹ or 1325 km³.yr⁻¹ on average) and extreme discharge ranging from 24,700 to 75,500 m³.s⁻¹ (Laraque et al., 2001; Spencer et al., 2012). This steady hydrological regime is due to the geographical position of the Congo River and its tributaries on both sides of the equator.

The concentration of total suspended sediment (TSS) in the Congo River is 26.3 mg.L⁻¹ on average (Coynel et al., 2005).

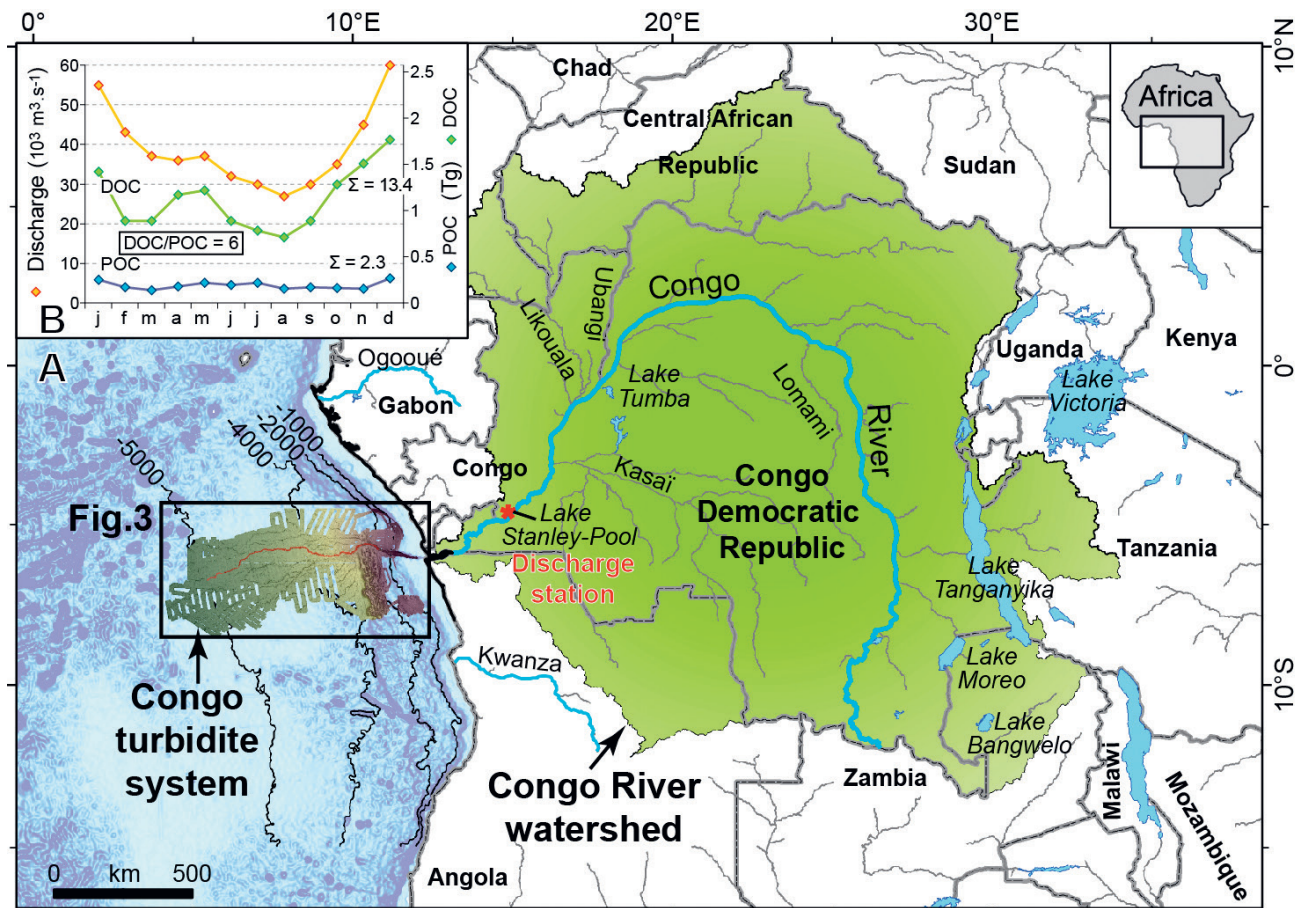


Figure 1. (A) The Congo sedimentary system from source (Congo River and its watershed) to sink (turbidite system) reprinted from Picot et al. (2016). (B) Hydrograph of the Congo River at the Brazzaville/Kinshasa station (outlet of the Stanley Pool, red star on the figure) with the temporal distribution of monthly water discharges (in $10^3 \text{ m}^3/\text{s}$), as well as Dissolved Organic Carbon and Particulate Organic Carbon quantity (both in Tg of carbon; Tg = 10^{12} g). The annual export of dissolved organic carbon (DOC) and particulate organic carbon (POC) is given as the sum on the right. Data from Kinga-Mouzéo (1986).

These low TSS levels are due to the convergence of many factors (Seyler et al., 2006):

- 1- the low overall altitude of the Congo watershed, leading to a limited production of sediments by mechanical erosion;
 - 2- the presence of numerous lakes along its stream and those of its tributaries, trapping part of the TSS and the bed load. It is noteworthy that the bed load discharge has not been estimated for the Congo River;
 - 3- the extensive vegetation cover that also limits erosion.
- Indeed, the Congo watershed is mainly covered by evergreen forest (50% of the total area) surrounded by savannah. Swamp forests cover the Central Depression (also called “Cuvette congolaise”), in which most of the forests are flooded during the wet season.

Although the TSS concentration is low, the Congo River delivers yearly between 30 to 70 Tg (average 40 Tg) of sediment to the Atlantic Ocean (Wetzel, 1993). A significant part of the TSS is composed of particulate organic matter (POC) as the Congo ranks fifth in term of annual POC flux to the oceans with an export reaching $\sim 2 \text{ Tg C}\cdot\text{yr}^{-1}$ (Coynel et al., 2005, Fig. 1B). The Congo River presents a high concentration of POC, ranging 6–7.5% (Spencer et al., 2012, 2014), compared to $\sim 1\%$ for the Amazon River and $\sim 0.2\%$ for Ganges-Brahmaputra River (Seiter et al., 2004).

2.2. Congo mouth and surface dispersion of the riverine flow

At its mouth, the discharge of the Congo River is distributed between a surface plume and a bottom current that flows into a canyon connected to the estuary (Fig. 2). The incision of the canyon head enables marine waters to invade the estuary (Cadée, 1984; Eisma & Kalf, 1984). A thin layer of fresh-water overflows this saline-water intrusion, travels north-westwards, and extends as a plume, up to 800 km from the coast. This surface layer is rich

in fine sediment, including POC, as well as in nutrients delivered by the Congo River or resulting from the remineralization of dissolved organic matter. Consequently, annual primary production in this area of the Atlantic Ocean reaches $400 \text{ g C}\cdot\text{m}^{-2}$ (Antoine et al., 1996). Locally, wind-driven seasonal upwellings increase the primary production levels up to $700 \text{ g C}\cdot\text{m}^{-2}$ (Antoine et al., 1996; Schneider et al., 1997). However, moving away from the coast, organic carbon concentration decreases gradually until the plume is no longer discernible (Cadée, 1984). All over the extent of the plume, a fine mixture of terrestrial POC and newly formed marine POC settles towards the seafloor (Fig. 2). Unfortunately, the relative proportion of marine *versus* terrestrial POC in the plume is unknown.

2.3. Submarine turbidite system

The 40 Tg of TSS annually delivered by the Congo River feed one of the largest mud-rich turbidite systems in the world, with a total surface area reaching $\sim 300,000 \text{ km}^2$. $21,400 \text{ km}^2$ of this surface area correspond to the canyon and deep-sea channel-levee system where turbidite sedimentation is active and $280,000 \text{ km}^2$ correspond to abandoned channel where hemipelagic deposits prevails (Reading & Richards, 1994; Stow et al., 1996; Savoye et al., 2000). The Congo turbidite system constitutes the major depocenter of the south-eastern Atlantic Ocean (Fig. 1A) and is among the largest modern deep-sea fans in the world. This system is supplied by a single source-point, the head of the canyon. Consequently, the turbidite system is active regardless of the sea level changes (Droz et al., 1996, 2003; van Weering & van Iperen, 1984). The occurrence of turbidity currents in the canyon was evidenced by submarine cable breaks (Heezen et al., 1964) and direct records during long-term moorings (Khrifounoff et al., 2003; Vangriesheim et al., 2009; Azpiroz-Zabala et al., 2017). Turbidity currents are confined to a narrow corridor with steep

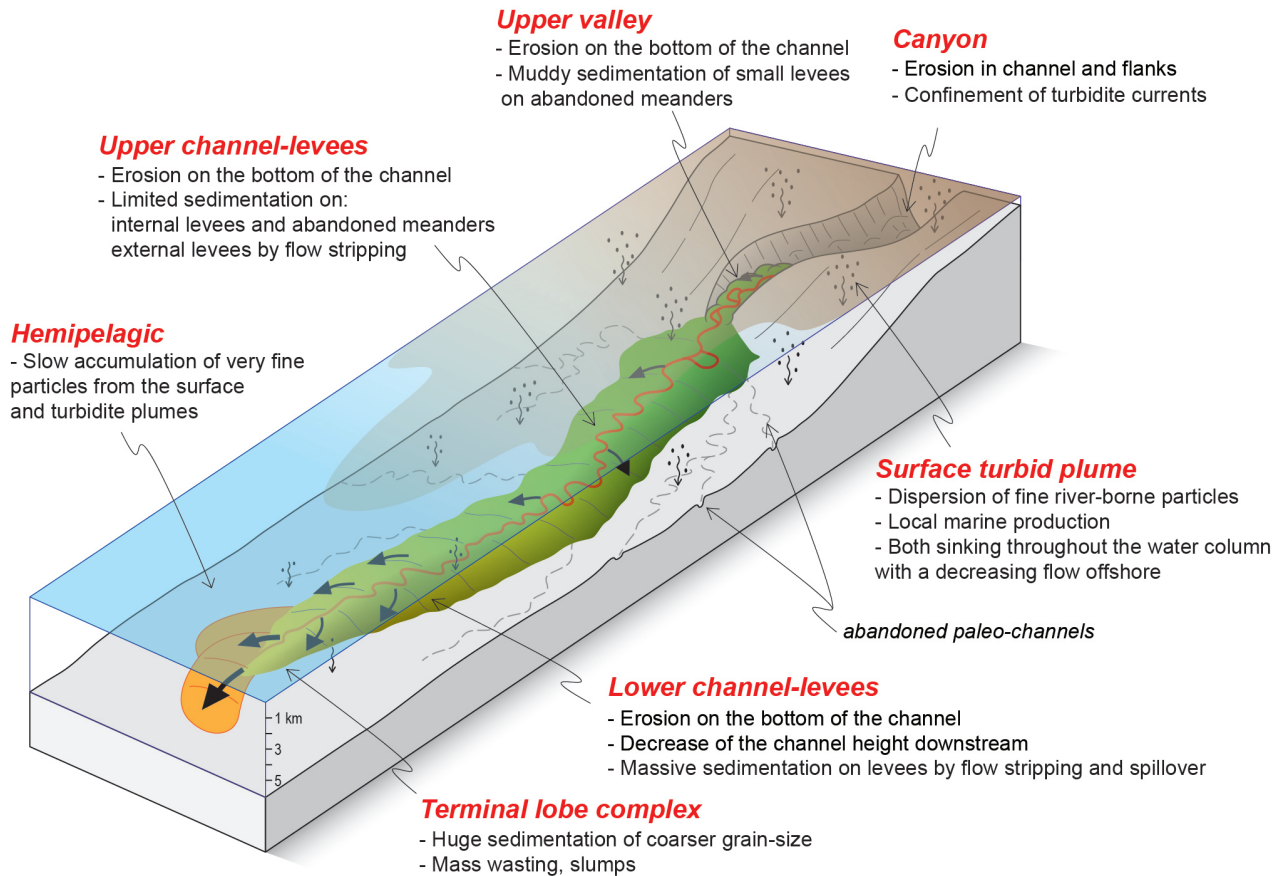


Figure 2. Sedimentary processes in the surface and submarine environment off the Congo River mouth with the main characteristics of the different environments of the turbidite system (inspired from Babonneau, 2002).

side walls (Fig. 2) and continue downstream until the canyon disappears around 2000–2300 m depth. Then, a transition zone starts linking the canyon to the channel-levees area, where transport and depositional processes occur simultaneously (Babonneau et al., 2002). At the end of the channel where the turbidity currents finish their course, the sediment that reaches these abyssal depths accumulates onto the terminal lobe complexes (Savoye et al., 2009; Mulder & Etienne, 2010; Dennielou et al., 2017). Sediment collapse along the canyon and the channel seem to be a common trigger mechanism of the turbidite flows. Although hyperpycnal flows have never been monitored in the Congo submarine system, they may be a subordinate triggering process. The recurrence of turbidity currents in the canyon may reach up to 60 per century (Heezen et al., 1964), but is much lower in the distal part of the turbidite system, ca. 2 to 10 per century (Savoye et al., 2009; Dennielou et al., 2017).

The submarine channel, its adjacent thick muddy levees and distal lobe complex represent the three basic architectural elements of the turbidite system. The entire Congo deep-sea fan results from the growth, avulsion and death of tens of such architectural elements, representing 80–90% of the sediment thickness according to seismic investigations (Droz et al., 2003; Savoye et al., 2009). Unconformable mass-transport deposits are less frequent, representing the remaining (~ 10–20%) of the total sediment (Droz et al., 2003).

As observed in many turbidite systems, only one channel-levees-lobe continuum is active at any given time (Droz et al., 1996; Savoye et al., 2000), the abandonment of the active channel is achieved through avulsion of the feeder channel that can be a gradual but generally non-reversible process (Droz et al., 2003; Picot et al., 2019). More than 80 inactive palaeo-channel-levees-lobe systems have been identified in the Quaternary Congo turbidite system (Picot et al., 2016; Savoye et

al., 2000, 2009). The modern active canyon-channel-lobe system extends 760 km westward off the Congo-Angola margin (Figs 1A and 3). Therefore, the Congo River source-to-sink system is a channelized continuum, from the watershed to the deepest distal zones of the deep-sea fan. This is particularly suitable for calculating sedimentary budgets.

3. Summary of recent studies on the Congo deep-sea fan

The Congo turbidite system was thoroughly studied during the last 25 years, particularly by the French community. Sixteen oceanographic campaigns took place in this area (Cochonat & Robin, 1992; Cochonot, 1993, 1998; Savoye, 1998; Savoye & Ondreas, 2000; Sibuet, 2001a, 2001b; Khripounoff, 2003; Marsset & Droz, 2010; Olu, 2011; Rabouille, 2011) allowing the acquisition of several thousands of kilometres of seismic lines, 250,000 km² of swath bathymetry survey, deployment moorings with sediment traps and current-metres, dives with submarine vehicles, sediment cores and *in situ* geochemical measurements. Additionally, numerous sedimentological and organic geochemical data were obtained during the shore-based studies on the 145 sediment cores collected in different parts of the Congo turbidite system, from the canyon head to the terminal lobe complex, by ca. 5000 m of water depth (Droz et al., 1996, 2003; Gervais et al., 2001; Babonneau, 2002; Babonneau et al., 2002, 2004, 2010; Ferry et al., 2004; Migeon et al., 2004; Bonnel, 2005; Treignier, 2005; Marsset et al., 2009; Rabouille et al., 2009, 2017a, 2017b; Baudin et al., 2010, 2017a, 2017b; Picot, 2015; Stetten et al., 2015; Picot et al., 2016, 2019; Croguennec et al., 2017; Méjanelle et al., 2017; Pastor et al., 2017; Pozzato et al., 2017; Schnyder et al., 2017; Taillefert et al., 2017). The resulting data allows a good description and understanding of the entire Congo turbidite system.

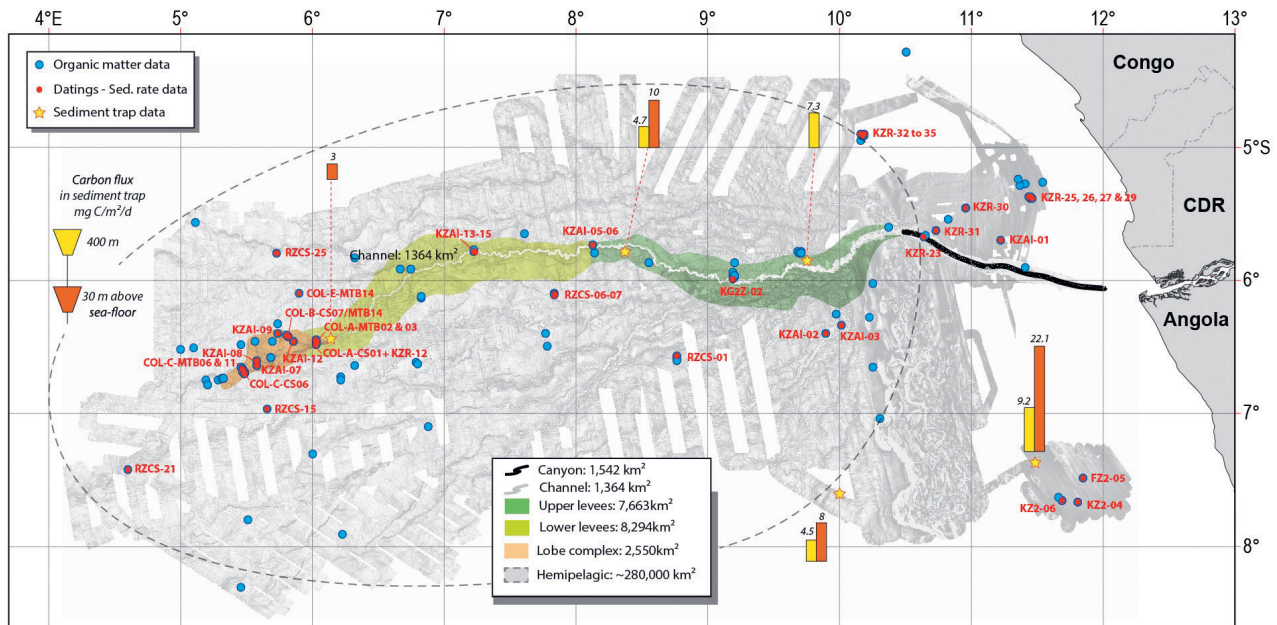


Figure 3. Location of cores collected and studied along the Congo active turbidite system and in hemipelagic environments bordering it; in green: channel-levees system and in light brown: lobe complex area. Red dots indicate core having been dated by radioisotopes (see Table 1). Yellow stars are the five mooring sites of sediment traps. Average carbon fluxes (in mg C/m²/d) measured at 30 m and/or 400 m above seafloor are given for each mooring site.

3.1. Sedimentary architecture

The channel-levees-lobe architecture is a fundamental element of the channelized continuum within the Congo deep sea fan (Figs 2 and 3). General characteristics of each compartment of this elemental organisation are summarised hereafter.

At the exit of the canyon, a channel entrenchment is always observed both in the present-day active channel (Babonneau et al., 2004) and in buried channels (Picot et al., 2016). This entrenchment enhances the confinement of turbidity currents and allows them to maintain their energy far downstream in the channel. Consequently, the channel is mainly a zone of bypass characterized by no net deposition. Only gravel and sand are deposited in it, as revealed by a high amplitude backscatter image, ROV direct observations and some short cores having penetrated the channel bottom (Savoye et al., 2009; Dennielou et al., 2017).

The channel morphology is characterized by meandering, which shows a decrease of sinuosity downstream (Babonneau et al., 2004). The upper part of the turbidity current overflows more effectively the channel flanks in meander portion of the channel, and consequently builds levees. The 2D extent of the levees was delimited by the analysis of both bathymetric and acoustic backscatter maps (Babonneau et al., 2004; Migeon et al., 2004). Levees occur on both sides of the channel with a relatively symmetrical morphology and a lateral extent decreasing downslope from 50 km to 10 km (Babonneau et al., 2002, 2004; Savoye et al., 2000, 2009). Levees form lens-shaped accumulations of overbank turbidites, dominantly composed of fine-grained sequences of silts and clays, supplied by overflows of the upper part of turbidity currents (van Weering & van Iperen, 1984; Gervais et al. 2001; Migeon et al. 2004). Secondary architectural elements on Congo levees include large sediment waves (Migeon et al., 2004) that are related to the dynamics of overflowing turbidity currents. Two different overflow processes are involved in the construction of levees: flow-stripping corresponding to local overflows in meanders and overspill, which is continuous along the channel. Babonneau et al. (2002) distinguished an upper channel-levee area (between 3300 and 4100 m depth) and a lower channel-levee area (between 4100 and 4750 m depth) according to the height of the channel entrenchment and the slope degree. In the upper channel-levee area, muddy-clayey turbidites predominate, because the levee relief prevents spillover of silt and sand carried in the bottom part of the turbidite current. However, the presence of thin silty layers suggests that more energetic and thicker billows carrying coarser

suspended particles may sometimes overflow from the channel and levee flanks. In the lower channel-levee area, the channel relief becomes less than 100 m leading to an increase of turbidite beds in the levee deposits with coarser individual turbidite sequences. These morphological limits between lower and upper levees are supported by sedimentation rates data (Savoye et al., 2009), which show that a major increase in accumulation rate appears between km 720 and km 850 along the path of the channel.

At the termination of the present-day active channel lies a cluster of lobes (Fig. 3), called the lobe complex by Marsset et al. (2009). The lobe complex lies 760 km off the Congo River mouth in the abyssal plain between 4740 and 5030 m depth. Successively Droz et al. (2003), Babonneau (2002) and Bonnel (2005) provided a general description of the terminal lobes whereas Dennielou et al. (2017) focused on the structure, composition, and dating of the lobes belonging to the presently active system. The present-day active lobe complex (90 km long x 30 km width; 2525 km²) is subdivided into five 20 to 25 m-thick individual lobes that have prograded south-westward. The lobes are dominantly muddy, consisting mainly of clay to silty turbidites. Coarse sediments (sand) are restricted to channel-fills including the small distributive channels on the lobes and represent ca. 13% of the deposits of the lobe complex (Dennielou et al., 2017). *In situ* mass wasting, slumps and debris characterize the whole lobe complex (Croguennec et al., 2017; Dennielou et al., 2017). High-resolution bathymetry using ROV shows extensive block on the edges at the channel mouth indicating that sliding occurs continuously in the lobe build-up. Mass wasting is generated by very high accumulation rates, over-steepening and erosion along the channels. The branching of the lobe complex is probably triggered when the slope gradient becomes flat and when turbidity currents flow on the higher gradient of a lobe side. Nevertheless, when a new lobe develops, the abandoned lobes continue to collect significant turbiditic deposits via spillover. Consequently, the whole lobe complex remains sedimentary active, at least for several centuries up to a few millennia.

3.2. Seabed chronologies and sedimentation rates

The geochronologies and sediment accumulation rates of 43 cores were determined by a combination of ¹⁴C, ²¹⁰Pb and/or ¹³⁷Cs (Savoye et al., 2009; Stetten et al., 2015; Rabouille et al., 2017b; Picot et al., 2019). These cores were collected at water depths ranging from 502 to 5178 m. These cores are located on continental slope adjacent to the canyon, on terraces inside the canyon, on

Table 1. List of cores collected and dated during the last 20 years of the French exploration of the Congo deep sea fan allowing estimates of the sedimentation rate in the different depositional environments. GC: gravity core and MTB: multitube for the type of corer. Information about sediment cores are available on IGSN webpages (e.g. <http://igsn.org/BFBGX-54257>).

Leg name	Station	Core type	Latitude °S	Longitude °E	Water depth [mbsf]	Depositional environment	Dating methods	Sedimentation rate [cm/ka]	IGSN reference http://igsn.org/	Reference(s)
Congolobe										
	COL-A-CS01	GC	-6.4629	6.0319	4755	lobe	137Cs, 210Pb	1000	BFBGX-54257	Rabouille et al., 2017b; 2019
	COL-A-MTB02	MTB	-6.4599	6.0346	4759	lobe	137Cs, 210Pb	1000		Rabouille et al., 2017b; 2019
	COL-A-MTB03	MTB	-6.4701	6.0369	4764	lobe	137Cs, 210Pb	1000		Rabouille et al., 2017b; 2019
	COL-B-CS07	GC	-6.4268	5.8262	4822	lobe	137Cs, 210Pb	300	BFBGX-54273	Rabouille et al., 2017b; 2019
	COL-B-MTB12	MTB	-6.4269	5.8264	4823	lobe	137Cs, 210Pb	300		Rabouille et al., 2017b; 2019
	COL-C-CS06	GC	-6.6991	5.4888	4954	lobe	137Cs, 210Pb	22000	BFBGX-54271	Rabouille et al., 2017b; 2019
	COL-C-MTB011	MTB	-6.6991	5.4888	4961	lobe	137Cs, 210Pb	12000		Rabouille et al., 2017b; 2019; Stetten et al., 2015
	COL-C-MTB06	MTB	-6.6710	5.4733	4951	lobe	137Cs, 210Pb	12000		Stetten et al., 2015
	COL-E-MTB14	MTB	-6.0982	5.9080	4750	lobe	137Cs, 210Pb	50		Rabouille et al., 2017b; 2019
Guinness	KG2Z-02	GC	-5.9903	9.2008	3490	levee	AMS 14C	58	BFBGX-90990	Savoie et al., 2009
Zaiango										
	KZAI-01	GC	-5.7031	11.2335	816	hemipelagic	AMS 14C	23	BFBGX-86532	Savoie et al., 2009
	KZAI-02	GC	-6.4033	9.9016	3412	hemipelagic	AMS 14C	14	BFBGX-86531	Dalibard et al., 2014
	KZAI-03	GC	-6.3456	10.0228	3407	hemipelagic	AMS 14C	5	BFBGX-86529	Savoie et al., 2009
	KZAI-05	GC	-5.7416	8.1381	4012	levee	AMS 14C	79	BFBGX-86527	Savoie et al., 2009
	KZAI-06	GC	-5.7350	8.1371	4150	levee	AMS 14C	58	BFBGX-86526	Savoie et al., 2009
	KZAI-07	GC	-6.6431	5.5800	4934	lobe	137Cs, 210Pb, AMS 14C	2500	BFBGX-86518	Savoie et al., 2009; Rabouille et al., 2019
	KZAI-08	GC	-6.6133	5.5800	4931	lobe	137Cs, 210Pb	700	BFBGX-86525	Rabouille et al., 2017b; 2019
	KZAI-09	GC	-6.4066	5.7500	4854	lobe	137Cs, 210Pb	400	BFBGX-86524	Rabouille et al., 2017b; 2019
	KZAI-12	GC	-6.4655	5.8633	4813	lobe	AMS 14C	50	BFBGX-86520	Rabouille et al., 2017b
	KZAI-13	GC	-5.7883	7.2315	4347	levee	AMS 14C	430	BFBGX-86522	Savoie et al., 2009
	KZAI-14	GC	-5.7848	7.2330	4343	levee	AMS 14C	276	BFBGX-86519	Savoie et al., 2009
	KZAI-15	GC	-5.7770	7.2365	4433	channel	AMS 14C	6	BFBGX-86517	Savoie et al., 2009
	FZ2-05	GC	-7.4908	11.8600	908	hemipelagic	Carbonate fluctuation	7	BFBGX-86558	unpublished data
	KZ2-04	GC	-7.6700	11.8150	1227	hemipelagic	Carbonate fluctuation	6	BFBGX-86555	unpublished data
	KZ2-06	GC	-7.6625	11.6990	1349	hemipelagic	Carbonate fluctuation	7	BFBGX-86546	unpublished data
Zairov										
	KZR-12	GC	-6.4826	6.0391	4737	lobe	AMS 14C	446	BFBGX-86509	Savoie et al., 2009
	KZR-23	GC	-5.6765	10.6400	2187	canyon	AMS 14C	135	BFBGX-86477	Savoie et al., 2009
	KZR-25	GC	-5.3810	11.4463	597	hemipelagic	Carbonate fluctuation	21	BFBGX-86472	unpublished data
	KZR-26	GC	-5.3850	11.4705	502	hemipelagic	Carbonate fluctuation	25	BFBGX-86483	unpublished data
	KZR-27	GC	-5.3823	11.4575	550	hemipelagic	Carbonate fluctuation	15	BFBGX-86467	unpublished data
	KZR-29	GC	-5.4598	10.9635	1496	hemipelagic	AMS 14C, Carb. Fluct.	6.5	BFBGX-86465	unpublished data
	KZR-30	GC	-5.4605	10.9701	1490	hemipelagic	Carbonate fluctuation	4	BFBGX-86479	unpublished data
	KZR-31	GC	-5.6350	10.7428	1861	hemipelagic	AMS 14C, Carb. Fluct.	7.5	BFBGX-86504	unpublished data
	KZR-32	GC	-4.9113	10.1916	2804	hemipelagic	Carbonate fluctuation	4.5	BFBGX-86497	unpublished data
	KZR-33	GC	-4.9150	10.1878	2817	hemipelagic	Carbonate fluctuation	8.5	BFBGX-86507	unpublished data
	KZR-34	GC	-4.9498	10.1616	2839	hemipelagic	AMS 14C, Carb. Fluct.	16.5	BFBGX-86468	unpublished data
	KZR-35	GC	-4.92116	10.1791	2833	hemipelagic	Carbonate fluctuation	8.5	BFBGX-86488	unpublished data
Reprezai										
	RZCS-01	GC	-6.5695	8.7681	4020	hemipelagic	AMS 14C	15	BFBGX-86912	Picot et al., 2019
	RZCS-06	GC	-6.1040	7.8396	4166	hemipelagic	AMS 14C	1	BFBGX-86917	Picot et al., 2019
	RZCS-07	GC	-6.1185	7.8432	4163	hemipelagic	AMS 14C	2	BFBGX-86918	Picot et al., 2019
	RZCS-15	GC	-6.9739	5.6601	4973	hemipelagic	AMS 14C	2	BFBGX-86926	Picot et al., 2019
	RZCS-21	GC	-7.3872	4.6301	5178	hemipelagic	AMS 14C	4	BFBGX-86932	Picot et al., 2019
	RZCS-25	GC	-5.7952	5.7306	4843	hemipelagic	AMS 14C	1	BFBGX-86936	Picot et al., 2019

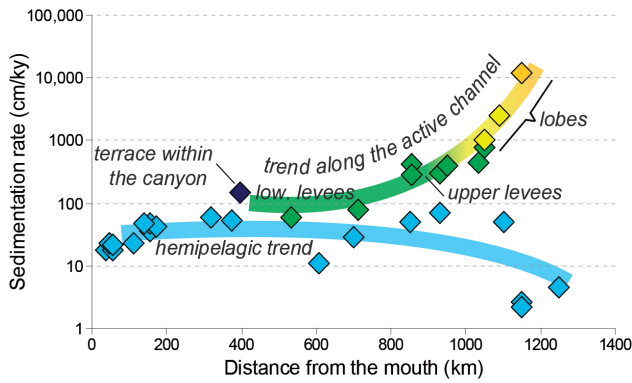


Figure 4. Evolution of the sedimentation rates (in cm/ky) in recent deposits along the canyon/channel-levees/lobes continuum and in surrounding hemipelagic environments influenced by the Congo turbidite system according to the distance from the river mouth.

the levees, in the channel and on the lobe complex, as well as far away from the present-day active channel where hemipelagic sedimentation prevails (Table 1; Fig. 3). In addition to these data, 33 sites derived from the study of Jansen et al. (1984) and 2 sites (GeoB1401 and GeoB1008) studied respectively by Haesse et al. (1997) and Schneider et al. (1994) were also considered in the present study for estimating sediment accumulation rate in the different parts of the Congo turbidite system. Because most of these additional sites are located in the hemipelagic domain, a mean sedimentation rate for the isotopic stage 1 was chosen as representative. The choice of isotopic stage 1 for the hemipelagic sites is justified because the turbidite system of the Congo River shows substantial changes in its architecture with respect to glacial-interglacial cycles (Marsset et al. 2009). Restricting our study to interglacial sediment is therefore cautious. Considering a constant hemipelagic sedimentation rate is certainly an approximation but in the absence of ultra-high resolution data, this hypothesis is the only acceptable one.

Accumulation rates on the continental slope adjacent to the canyon are low (23 cm.k.a^{-1} to 37 cm.k.a^{-1}) whereas accumulation rate may reach 130 cm.k.a^{-1} on terraces inside the canyon (Babonneau et al. 2004). This relatively high accumulation rate suggests a probable contribution of dilute sedimentary billows from the canyon and/or the rapid and intense sinking of terrigenous particles from the surficial turbid plume. Along the channel-levees system, the accumulation rates tend to increase downstream, and are negatively correlated to the channel height

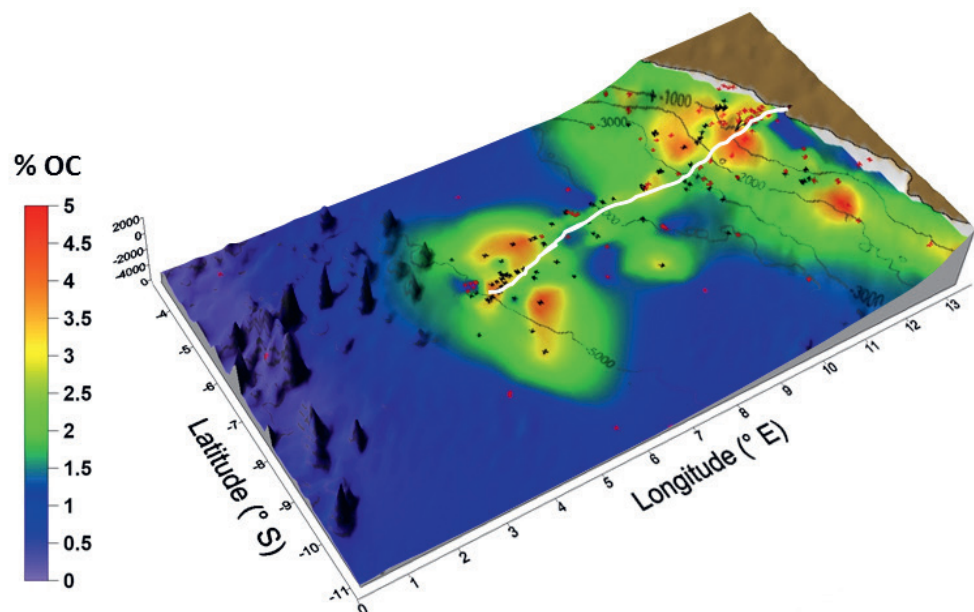
and positively correlated to the distance along the channel. Although the accumulation rates within the cores in the levees show a strong variability, related to the discontinuous nature of the turbiditic supply, the accumulation rates range between 50 cm.k.a^{-1} in the upper channel-levees area and 800 cm.k.a^{-1} in the lower channel-levees area (Fig. 4). Sedimentation rates recorded in the lobe complex are much higher. Very large excess in ^{210}Pb and ^{137}Cs over metres of sediment lead to sedimentation rates $>2.5 \text{ cm.yr}^{-1}$ (25 m.k.a^{-1}) and even up to 10 to 22 cm.yr^{-1} , which is an ultra-high accumulation rate for sediments at 5000 m deep (Stetten et al., 2015; Rabouille et al., 2017b). These extremely high rates are related to the nature of the lobe complex at the end of the main channel, where most of the material carried by the present turbidite flows accumulates. Compared to accumulation rates in the pelagic abyssal plain, the values reported for the Congo deep-sea fan are therefore 100 times larger on the active levees and 1000 times larger on the terminal lobe (Fig. 4). The present-day active lobe complex ($\sim 2525 \text{ km}^2$; $\sim 90 \text{ km}^3$ of accumulated sediments) could have been deposited during the Late Holocene (Dennielou, 2002) or even a shorter time interval of ca. 4000 years (Picot et al., 2016).

3.3. Organic matter content in recent sediments

The intensive coring during the oceanographic campaigns carried out on the Congo deep-sea fan zone offers the opportunity to analyse the organic matter content of the sediments deposited on the seafloor as well as of the particles sinking in the water column and collected at different depths during long-term sediment trap moorings. The first studies focused on sediment traps and the kinetics of organic matter remineralization. Treigner et al. (2006) studied *n*-alcohol biomarkers from sediment trap samples collected 30 m and 400 m above the seafloor by 4000 m depth, which captured a turbiditic event, as well as surficial sediments on the levee 9 months after the turbiditic event. They showed that the organic matter of the turbidity current suspension has a strong terrigenous signal compared with the composition of the particles sinking from surface in a hemipelagic reference area. The terrestrial origin of the organic matter, as revealed by *n*-alcohol distribution, is also visible in the surficial sediments of the levee built by accumulation of muddy turbidite, showing a C_{org} content around 2.2% . Although the organic matter delivered by turbidity currents is already altered and despite the predominance of higher plant compounds resistant towards degradation, it is further degraded on the seafloor.

The rate of carbon remineralization near the active channel and 200 km away was calculated by Rabouille et al. (2009, 2019) using a combined approach. Vertical organic carbon fluxes were measured using long-term sediment trap moorings. Organic carbon accumulation rates in the sediment were derived from sedimentation

Figure 5. Map of the C_{org} content (wt% of dry and desalted sediment) in topmost sediments ($<3 \text{ cm}$ depth) in the Southeastern Atlantic Ocean off the Congo River (modified from Baudin et al., 2017a). Sediments related to the Congo turbidite system are significantly enriched in C_{org} until the abyssal plain. The white line correspond to the path of the present-day active turbidite channel. Black dots correspond to the core sites reported on Figure 3, and red dots correspond to core sites from previous studies (see Baudin et al., 2017a for details).



rates estimated by short-lived radioisotopes (^{210}Pb and/or ^{137}Cs) and organic carbon content of the sediment. Organic carbon recycling was estimated using a combination of *in situ* benthic chambers and microprofiler measurements, which provided total and diffusive oxygen uptake as well as oxygen profiles in porewaters as tracers of benthic carbon recycling (Rabouille et al., 2009). Results show a decreasing recycling of organic carbon with increasing water depth, except for the lobe complex area where recycling is 5–6 times more active, because of the extremely high organic carbon deposition in that area. Despite the intense recycling, only ~15% of the terrigenous organic matter is remineralized on the seafloor whereas ~85% is buried and constitute a large sink of organic carbon that accounts for an accumulation of $0.35 \text{ Tg C.yr}^{-1}$ (Rabouille et al., 2009, 2019).

Maps of organic geochemical characteristics (C_{org} content, $\delta^{13}\text{C}_{\text{org}}$, C/N, Rock-Eval pyrolysis) of the topmost sediments provide an overview of POC distributions and potential reactivity or degree of reworking at the scale of the Congo margin (Fig. 5; Baudin et al., 2017a). The downslope trend in C_{org} content and organic matter composition points to a primary control of the turbidity currents on the supply and accumulation of organic matter. The source of organic matter, estimated using carbon stable isotope signature, is clearly related to both bathymetry and the distance from the active turbidite channel. A high content of terrestrial organic matter is observed downslope along the active turbidite channel of the Congo deep-sea fan. This is accompanied by a very large C_{org} concentration (up to 4%) in the terminal lobe complex (Fig. 5). Detailed organic geochemical investigations, including molecular signatures and palynofacies observations, were conducted in the upper and lower channel-levee areas (Baudin et al., 2010) and in the terminal lobe complex (Stetten et al., 2015; Baudin et al., 2017b; Méjanelle et al., 2017; Pruski et al., 2017; Schnyder et al., 2017). All geochemical and palynological proxies suggest that at least 80–90% of the organic matter preserved in marine sediment along the turbidite channel has a terrestrial origin. All the analyses confirm that the origin of organic matter is a mixture of terrestrial higher-plant debris, soil organic matter and deeply oxidized phytoplanktonic material. Nevertheless, variations in the contributions of biomarkers from higher plants, ferns, bacteria and angiosperms, indicate a heterogeneous contribution of the soil and vegetation detritus delivered by the Congo River (Méjanelle et al., 2017). Fine structures of higher plant, cuticle fragments and vegetal cellular material are generally well preserved, emphasizing the efficiency of turbidity currents to rapidly transfer terrestrial organic matter to the seafloor (Schnyder et al., 2017). The palynofacies data reveal a general sorting by density/buoyancy of the organic particles from the channel toward the levees. Despite these subtle variations, the organic matter content distribution appears relatively homogeneous at different scales, from a single cm- to dm-thick turbiditic event to several m-long core all along the turbidite system. Changes in accumulation rates have a limited effect on the quantity and quality of preserved organic matter, whether in channel-levees system (Baudin et al., 2010) or in the terminal lobe zone (Stetten et al., 2015; Baudin et al., 2017b; Schnyder et al., 2017). Consequently, it was possible to consider POC as a conservative parameter of the system and to use it to compute a budget of organic carbon in a S2S approach.

4. S2S approach

4.1. Methodology

Although the Congo River delivers 6 times more dissolved organic carbon compared to POC (Fig. 1A), we focus here only on POC because it represents the fraction that is ultimately buried and has the potential to enter the long-term carbon cycle. POC comprises heterogeneous mixtures of organic particles from different sources, having a range of ages and reactivities (Hedges & Keil, 1995; Blair et al., 2010). It includes fragments of terrestrial vascular plants (e.g. leaves, wood, spores and pollen grains), remains of freshwater and marine algae, all fractions that have been relatively recently fixed via photosynthesis and referred to as modern carbon. POC also comprises a portion of primary production which is recycled and aged during its storage in soils

and sediments for up to thousands of years, and referred to as old carbon. The combination of these two sources of POC, fresh and altered, leads to a continuum of age and reactivity of organic matter in sedimentary systems. Moreover, POC sometimes includes much older and more recalcitrant organic particles provided by the erosion of sedimentary and metamorphic rocks, referred to as fossil or petrogenic carbon (Copard et al., 2006; Galy et al., 2007; Blair et al., 2010; Galy & Eglinton, 2011). Here, in the case of the Congo River, this later source can be neglected because it is very limited (<2% relative to POC, Galy et al., 2015) compared to the other two forms of POC.

In our S2S approach, we consider that the POC flux, as determined at the Brazzaville/Kinshasa station (Spencer et al., 2012, 2014), corresponds to the flux delivered in the Atlantic Ocean by the Congo River. Indeed, it is out of our purpose to detail the changes of this flux between this part of the river and the river outlet. Readers interested in the different sources of carbon in the Congo watershed are referred to previous studies by Coynel et al. (2005) or Spencer et al. (2012, 2014). During the last 25 years, the POC fluxes have been estimated by different authors, using different techniques, at the Brazzaville/Kinshasa station with a certain variance in the estimate of the annual Congo River export. The 1.9 to 2 Tg POC.yr^{-1} reported by Coynel et al. (2005) is a mean calculated value of the exported POC flux if we consider the variability of different computations, ranging from $1.2 \text{ Tg POC.yr}^{-1}$ (Probst et al., 1994) to $2.3 \text{ Tg POC.yr}^{-1}$ (Kinga-Mouzéo, 1986), $1.5 \text{ Tg POC.yr}^{-1}$ for Cadée et al. (1984) and $1.6 \text{ Tg POC.yr}^{-1}$ for Seyler et al. (1995). The estimate of 1.9 Tg made by Coynel et al. (2005) is preferred because it is calculated over 6 hydrological annual cycles while the Kinga-Mouzéo and Seyler estimates are calculated over one single hydrological year (1976 and 1992, respectively). However, taking into account these differences of flux estimates, we can calculate a standard deviation of $\pm 0.4 \text{ Tg C.yr}^{-1}$ for the annual POC flux delivered by the Congo River to the Atlantic Ocean.

Once this influx has been established, our S2S approach is to determine the offshore deposition flux of the terrestrial POC delivered by the Congo River. This is done by estimating the terrestrial POC flux that is deposited in surface sediments for a period of time ranging between a decade to a century, in the different parts of the turbidite system, as reported in Figure 2. By knowing the surface area of the different depositional environments, their sediment accumulation rates and their average organic contents, it is possible to calculate a Mass Accumulation Rate (MAR) of C_{org} . If we have information on the type of organic carbon (marine *versus* terrestrial), it is possible to calculate burial of terrestrial POC. In order to reconstruct the deposited flux, it is necessary to sum up accumulation and remineralization for the terrestrial and marine fractions (see Rabouille et al., 2019). The part of the marine primary production reaching the seafloor is very limited as revealed by the analysis of sediment traps that have been deployed in the area for one to several years. Moreover, the rate of remineralization of marine organic matter is high as demonstrated by Treignier et al. (2006). Consequently, the marine organic flux can be neglected in our computation. By contrast, the degradation rate of terrestrial POC on the seafloor was estimated ~16% in the lobe complex (Rabouille et al., 2019), a value rounded to 15% and extrapolated to all other parts of the turbidite system receiving directly their organic matter from the Congo River. Finally, it is important to have an idea of the representativeness and the uncertainties of the results by critically analysing our data set.

4.2. Sample dataset, representativeness and uncertainties

The 145 studied cores penetrated different depositional environments of the Congo turbiditic facies, including canyon-channel deposits (4 cores), levee deposits (16 cores) and lobe deposits (28 cores). The remaining 97 cores were recovered from hemipelagic deposits. The canyon-channel domain is clearly undersampled. In the lobes, the large geographical spread of sampling was necessary to estimate the variability in the heterogeneous environments of the terminal lobe complex (Dennielou et al., 2017; Rabouille et al., 2017b). The undersampling of the canyon-channel domain is related to the difficulty to core sandy facies. However, this undersampling has

a limited impact on our calculation because the canyon-channel area is mainly a zone characterized by no net or very limited deposition and by sandy facies lean of organic matter.

Several sources of uncertainty exist in our computational approach:

- Uncertainties on the surface areas of the different depositional environments. This source of uncertainty is negligible because the different domains of the active turbiditic system have been delimited with precision by Babonneau (2002), Dennielou et al. (2017) and Picot (2015) on the basis of seabed acoustic backscatter and sub-bottom profiler data.
- Uncertainties on sedimentation rates are much more important as several tools were used for coring (Table 1), including gravity coring in which the first centimetres or decimetres of the sediment are washed over when the tool penetrated the seafloor. Several geochronological methods have been also used, each of which presents uncertainties for these non-steady sedimentation regimes. For these two reasons, the uncertainty on sedimentation rates is approximately 30% of the estimated value, as mentioned by Rabouille et al. (2019).
- Uncertainties in the determination of organic carbon content of sediments is less than 5% of the measured C_{org} value using the Rock-Eval techniques on recent marine sediments (Baudin et al., 2015).
- One large uncertainty in the C-budget lies in the annual export of POC by the Congo River, which varies by a factor of two, ranging from 1.2 to 2.3 Tg C. With a chosen value of 1.9 ± 0.4 Tg C.y⁻¹, the uncertainty is of 20%.
- A final uncertainty concerns the vertical contribution of marine organic matter over the entire study area. Sediment trap analyses have shown that the vertical flux coming from the plume represents only one percent of the input from the river in the lobe zone (Rabouille et al., 2019). Moreover, this vertical organic flux comprises both marine and terrestrial organic matter. Treignier et al. (2006) confirm that marine organic matter is labile and therefore more intensely and quickly remineralized than that of terrestrial origin. If the POC from Congo River seems to be remineralized to about 15%, the remineralization of the marine one exceeds 95%. As a result this marine vertical flux is negligible and will not be taken into account in our calculations on the active turbidite system.

4.3. Basis of calculations

The flux of terrestrial OC buried yearly (in g C.m⁻².y⁻¹) is calculated as follows:

$$SR * (1-\phi) * \rho * \%OC * 10000 \quad (1)$$

where SR is the average sedimentation rate (in cm.y⁻¹), ϕ the porosity of the sediment, ρ the density of dry and desalted sediment (g.cm⁻³), and OC the fraction of terrigenous organic carbon in dry and desalted sediment (g C/100 g sediment). ρ is fixed to 2.5 g cm⁻³ for all recovered sediments. ϕ is 0.85 for the clayey-silty facies and 0.7 for the sandy facies.

The quantity of terrestrial OC accumulated per year in the study area is calculated by multiplying the flux by A the surface area (in m²) of each depositional environment:

$$SR * (1-\phi) * \rho * \%OC * 10000 * A \quad (2)$$

Total POC buried per year (in Tg C.y⁻¹) was calculated for average SR and average %OC values, as well as for the minimum and maximum of the standard deviation values of SR and %OC. Total budget of terrestrial OC buried per year of the entire study area (21,400 km²) is the sum of the total budget of terrestrial OC buried in the different depositional environments considered here.

5. Results and discussion

Sinks of POC in the turbidite environments

Results of our computations are reported in Table 2 for five different depositional environments: canyon, channel, upper levee, lower levee and terminal lobe. The channel is clearly an area with very low POC burial (0.001 Tg C.y⁻¹) due to the preponderant no net deposition and resulting low sedimentation rate. The canyon shoulders and the upper levees are areas of moderate POC burial, with values ranging from 0.02 to 0.06 Tg C.y⁻¹ (Table 2). The lower levees and lobes are areas of high to very high POC burial with both a value of 0.33 Tg C.y⁻¹. The lobe zone is clearly a large sink of the terrestrial POC exported by the Congo River, as already demonstrated by Rabouille et al. (2019). Interestingly, the lower levees domain represents a similar terrestrial POC sink because of the much larger surface area. Baudin et al. (2010) have shown that the quality of organic matter and its concentration did not vary between the upper and lower levees, despite a significant increase in sedimentation rates. As the sedimentation rate is 5 times greater in lower levees than in upper ones and all the other parameters being equal, the amount of accumulated POC varies to the same magnitude, with 0.06 Tg C.y⁻¹ for the upper levees and 0.33 Tg C.y⁻¹ for the lower levees.

According to our calculations, the average annual POC burial in the active turbidite system is estimated to 0.74 Tg C.y⁻¹ and range between 0.53 and 1.11 Tg C.y⁻¹ (Table 2). These values are very similar with an independent estimate of the annual export rates of POC in the canyon reported by Azpiroz-Zabala et al. (2017). These authors provide a strikingly similar range of 0.5 to 1.1 Tg C.y⁻¹ based on a completely different approach as they directly measure the canyon turbidity currents at 2000 m water depth.

It is possible to estimate the efficiency of the different depositional environment of the Congo turbidite system in trapping POC fluxes by calculating the percentage of the POC burial in each area of the system (Table 3 and Fig. 6). The lobes would accumulate about 45% of the total POC burial and the levees ~52%, whereas the canyon and channel would accumulate the remaining 3%. The terminal lobe domain is clearly a zone of mega-sink for terrestrial POC as already demonstrated by Rabouille et al. (2019). The current calculation allows incorporating the lower levees domain as another area of important POC sink.

Where is the missing part of POC flux?

The 0.74 Tg C buried yearly in the active Congo turbidite system represent the routing of 46% of the annual riverine POC flux

Table 2. Results of the calculation of POC annual burial fluxes in the different depositional environments of the Congo deep sea fan. Average annual burial fluxes per unit of surface (g C.m⁻².y⁻¹) were calculated from measured sedimentation rates, porosity and average POC content of surface sediments. The total POC burial fluxes (in Tg C.y⁻¹; 1 Tg = 10¹² g) were calculated according the surface covered by each depositional environment for the average, minimum and maximum values of uncertainties reported in the previous lines. Bold values are the sum of each line.

Depositional environment	Canyon	Channel	Upper levee	Lower levee	Lobe	Total
Surface area [km ²]	1542	1364	7663	8294	2525	21388
Sedimentation rate (min-max) [cm.y ⁻¹]	-	-	0.058 – 0.079	0.28 – 0.43	0.05 – 12	
Average Sed. Rate [cm.y ⁻¹]	0.13 ± 0.04	0.006 ± 0.002	0.065 ± 0.02	0.35 ± 0.10	1.0 ± 0.3	
Porosity [%]	0.85	0.70	0.85	0.85	0.85	
Corg [wt%, dry and desalted]	2.75 ± 0.14	2.0 ± 0.1	3.0 ± 0.15	3.0 ± 0.15	3.5 ± 0.2	
Terrestrial POC burial [g C.m ⁻² .y ⁻¹] average	13.9	0.9	7.3	39.7	131.3	
Total POC burial [Tg C.y ⁻¹] average	0.021	0.0012	0.06	0.33	0.33	0.74
Total POC burial [Tg C.y ⁻¹] minimum	0.020	0.0008	0.05	0.25	0.22	0.53
Total POC burial [Tg C.y ⁻¹] maximum	0.024	0.0017	0.07	0.42	0.60	1.11

Table 3. Mass balance for the total POC burial and their relative percentage in the different depositional environments of the Congo deep-sea fan. The relative percentage of carbon buried is also compared to the annual export of POC by the Congo River after remineralization. The terminal lobes area, covering ~12% of the surface of the deep sea fan, accumulates ~45% of the POC stored by the turbidite system itself or ~20.5% of the POC exported by the Congo River.

Depositional environment	Canyon	Channel	Upper levee	Lower levee	Lobe	Total
Surface area [km ²]	1542	1364	7663	8294	2525	21388
% surface	7.2%	6.4%	35.8%	38.8%	11.8%	
Total POC burial [Tg C.y ⁻¹]	0.02 ± 0.004	0.001 ± 0.0004	0.06 ± 0.01	0.33 ± 0.1	0.33 ± 0.2	0.74 ± 0.32
% C burial in the DSF	2.9%	0.2%	7.6%	44.5%	44.8%	
% C burial vs Congo R. input	1.3%	0.1%	3.5%	20.3%	20.5%	45.7%

(1.9 Tg C.y⁻¹) to the canyon and channel levee system assuming that 15% of the deposited flux is remineralized on the bottom (Rabouille et al., 2009, 2019). Taking into account the minimal and maximal estimates, the total POC buried yearly in the different parts of active turbidite system may range between 0.5 to 1.1 Tg C, that account for 33% and 69% of terrestrial carbon exported by the Congo River. A significant part of the POC riverine export is therefore not found in our S2S approach even though the Congo turbidite system is considered a relatively closed system. It is therefore necessary to question the fate of ca. 50% of the POC delivered by the Congo River.

A first reason lies certainly in our simplifications of this sedimentary system, which is quite complex. First of all, we applied a constant (15%) remineralization rate for terrestrial organic matter in the sediments, based on measurements performed *in situ* for a few hours at the terminal lobe complex (Rabouille et al., 2019). Extrapolating these values to areas where sediment accumulation rates are lower is uncertain. When the sedimentation rates are lower, the diffusion of oxygen from the bottom waters is more efficient and ultimately, even if the terrestrial organic matter is more refractory to remineralization, it is possible that the remineralization fraction exceeds 15%. Such a situation would tend to reduce the POC budget imbalance with less burial efficiency for the active turbidite system where sedimentation rate is lower. However, it should be noted that areas with low accumulation are limited in the active turbidite system and therefore are almost negligible in the carbon budget. The sedimentary system is also simplified as we consider a direct transport from the source to the depositional environment. In fact, there are many sediment reworking. Portions the canyon or channel edges collapse regularly supplying turbid flows and redistributing the sediment. The organic matter of these sediments therefore experiences several times a contact with oxidizing conditions. In the end, the remineralization rate is perhaps greater than 15%.

Secondly, in our S2S approach there are a number of uncertainties as discussed in section 4.2. Indeed, our carbon budget approach considers annual river discharge *versus* offshore

decadal to centennial averaged accumulation rates mass balances. Here again there may be a bias, because the annual POC inputs by the Congo River fluctuates according to the authors between 1.2 and 2.3 Tg C. The sedimentation rates are also very variable in the turbidite environments. Consequently, an accumulation rate measured over decades or a century and reported per year is not directly comparable to an annual export. However, as the Congo inputs were average over six different years by Coynel et al. (2005), the comparison seems more thorough.

A third and probably the most important reason for the calculated low proportion may be linked to a re-direction of particulate material and its trapping outside of the active turbidite system studied here. Indeed, the good agreement between our estimate and the estimate made by Azpiroz-Zabala et al. (2017) using the canyon flux suggest that the loss of material may be before the canyon. In other words, a lot of sediment may be bypassing the canyon on some undetermined time scale. Three additional areas should be considered as potential sink for terrestrial POC: (1) the hemipelagic domain, (2) the outer-shelf and the slope margin, and (3) the dispersion of particles by the surface plume far from the Congo River mouth. None of these three reservoirs was taken into account in our budget approach because the data are too scarce to allow calculations.

In the hemipelagic domain, sedimentation rate data are available but the determination of the proportion of terrestrial POC in the particles settling from the surface is missing, except in few sites where sediment traps were installed (Fig. 2). Indeed, the identification and quantification of organic matter sources, whether continental or marine, in marine hemipelagic and pelagic sediments are always difficult because several parameters influence the bulk and molecular characteristics of the preserved organic matter. Using the carbon isotopic signature of organic matter in topmost sediments in the studied zone, Baudin et al. (2017a) show that lighter isotopic ratios, suggesting an enrichment of terrestrial organic matter, are limited to a narrow (25–50 km) zone around the active turbidite system. This suggests that transfer and trapping of terrestrial POC are dependent of the turbidite phenomena and that marine organic matter becomes predominant away from the active channel, in hemipelagic sediment. Moreover, the low sedimentation rates and the low organic carbon content in hemipelagic sediments cannot generate a large sink for terrestrial POC, even if the hemipelagic surface is important.

By contrast, the zones of the outer platform and the top of the slope show enrichment in organic matter. If we examine the map of C_{org} in surface sediments off the Congo (Fig. 5), it is obvious that a zone with a 3–4% C_{org} is located around the canyon at water depths between 500 and 2000 m. There are limited data in this area to quantify the buried POC, but it is certainly a sink that should be taken into account because this zone shows sedimentation rates larger than average, ranging from 20 to 50 cm.ka⁻¹ (Fig. 4) and even more in some place (up to 100 to 200 cm.ka⁻¹, Rabouille et al., 2009).

Finally, the part of POC that is exported to the surface plume and potentially partly degraded along its course should not be neglected. Direct observations and satellite imagery show high turbidity in the Congo River plume extending north-westward from the African coast. If this leak significantly exports POC out of the study area, it would represent a way to balance the organic budget.

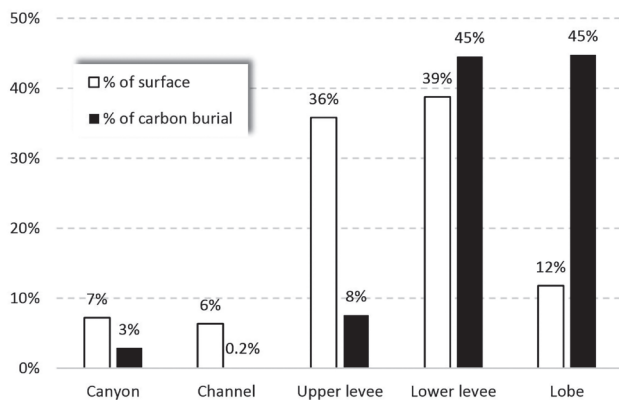


Figure 6. Comparison of the relative percentage of the surface covered by the different depositional environments related to the Congo turbidite system with the percentage of organic carbon buried in each area.

Despite these uncertainties, the POC balance budget for the Congo River presented here is as good as or even better than for other previously studied systems. Even sedimentary systems considered closed and of much smaller size than the Congo River, such as Taiwanese rivers (Hsu et al., 2014) or the Waipaoa River in New Zealand (Kuehl et al., 2016), show budget deficits of up to 75% outlining the difficulty to achieved budget calculations in sedimentary systems.

6. Conclusion

The source-to-sink concept applied to the Congo River terrestrial particulate organic matter is founded on our ability to correctly characterize and quantify present-day input and burial fluxes. Two distinct depocenters with high POC content are recognized on the Congo turbidite system: the terminal lobe complex at the end of the active channel, which accounts for 45% of the total POC burial despite its small surface (12% of the entire turbidite system), and the lower levees domain which accounts also for ~45% of the total POC burial for a surface of 39%. These two depositional environments are very efficient in trapping more than 43% of the annual POC delivered by the Congo River. Nevertheless, our sediment-budget considering offshore centennial accumulation rates compared to annual river discharge shows a ~50% deficit, suggesting that half of the total particulate organic matter delivered yearly by the Congo River watershed escapes the study area or is not correctly estimated in our S2S approach.

The study of organic carbon budget in the present-day Congo River system could potentially inform interpretations of the organic carbon buried in the geologic past. Climate changes obviously influence both the relative importance of biospheric and petrogenic organic carbon sources and the location of burial sites in the deep ocean. The main undetermined value for the glacial period is the organic carbon export by the Congo River and its preservation potential, which could be different at that time. For the location of burial sites, forward stratigraphic modelling may help in evaluating the effect of sea-level changes in the dispersion of terrestrial particulate organic matter in the Congo turbidite system.

The Congo River system is an analogue to glacial lowstand periods when other large and small rivers were closely connected to their canyons and riverine export to deep offshore was more efficient. It is expected that burial of POC in the turbidite system was much larger during glacial period. Thus, carbon-budget exercises similar to the one proposed in this paper are interesting for a better understanding of the carbon cycle over climatic and eustatic cycles.

7. Acknowledgements

We thank IFREMER and Total for providing samples from the Guinness, Zaiango, and Zairov campaigns. We are grateful to IFREMER/GENAVIR captains and crews for the Reprezaï, WACS and Congolobe campaigns onboard the R/V Pourquoi Pas? as well as Tania Marsset, Laurence Droz, and Karine Olu for leading the Reprezaï and WACS campaigns, respectively. We thank Sebastien Bertrand and Neal Blair for their comments on an earlier version of this paper. We acknowledge funding from ANR Congolobe (ANR Blanc SIMI5-6, n° 11BS56030), as well as institutional funding and support from IFREMER (BD), from CEA and CNRS (CR) and SU and CNRS (FB).

8. References

- Antoine, D., André, J.-M. & Morel, A., 1996. Oceanic primary production; 2. Estimation at global scale from satellite (coastal zone color scanner) chlorophyll. *Global Biogeochemical Cycles*, 10/1, 57–69. <https://doi.org/10.1029/95GB02832>
- Azpiroz-Zabala, M., Cartigny, M.J.B., Talling, P.J., Parsons, D.R., Sumner, E.J., Clare, M.A., Simmons, S.M., Cooper, C. & Pope, E.L., 2017. Newly recognized turbidity current structure can explain prolonged flushing of submarine canyons. *Science Advances*, 3/10, 12 p. <https://doi.org/10.1126/sciadv.1700200>
- Babonneau, N., 2002. Mode de fonctionnement d'un chenal turbiditique méandrique: Cas du système turbiditique actuel du Zaïre. Unpublished Ph.D. thesis, Université de Bordeaux I, Talence, 308 p.
- Babonneau, N., Savoye, B., Cremer, M. & Klein, B., 2002. Morphology and architecture of the present canyon and channel system of the Zaire deep-sea fan. *Marine and Petroleum Geology*, 19, 445–467. [https://doi.org/10.1016/S0264-8172\(02\)00009-0](https://doi.org/10.1016/S0264-8172(02)00009-0)
- Babonneau, N., Savoye, B., Cremer, M. & Bez, M., 2004. Multiple terraces within the deep incised Zaire valley (ZaiAngo Project): are they confined levees? In Lomas, S.A. & Joseph P. (eds), *Confined Turbidite Systems*. Geological Society, London, Special Publications, 222, 91–114. <https://doi.org/10.1144/GSL.SP2004.222.01.06>
- Babonneau, N., Savoye, B., Cremer, M. & Bez, M., 2010. Sedimentary architecture in meanders of a submarine channel: Detailed study of the present Congo turbidite channel (Zaiango Project). *Journal of Sedimentary Research*, 80, 852–866. <https://doi.org/10.2110/jsr.2010.078>
- Baudin, F., Disnar, J.R., Martinez, P. & Dennielou, B., 2010. Distribution of the organic matter in the channel-levees systems of the Congo mud-rich deep sea fan (West Africa). Implication for deep offshore petroleum source rocks and global carbon cycle. *Marine and Petroleum Geology*, 27, 995–1010. <https://doi.org/10.1016/j.marpetgeo.2010.02.006>
- Baudin, F., Disnar, J.R., Aboussou, A. & Savignac, F., 2015. Guidelines for Rock-Eval analysis of recent marine sediments. *Organic Geochemistry*, 86, 71–80. <https://doi.org/10.1016/j.orggeochem.2015.06.009>
- Baudin, F., Martinez, P., Dennielou, B., Charlier, K., Marsset, T., Droz, L. & Rabouille, C., 2017a. Organic carbon accumulation in modern sediments of the Angola basin influenced by the Congo deep-sea fan. *Deep-Sea Research II: Topical Studies in Oceanography*, 142, 64–74. <https://doi.org/10.1016/j.dsr2.2017.01.009>
- Baudin, F., Stetten, E., Schnyder, J., Charlier, K., Martinez, P., Dennielou, B. & Droz, L., 2017b. Origin and distribution of the organic matter in the distal lobe of the Congo deep-sea fan – A Rock-Eval survey. *Deep-Sea Research II: Topical Studies in Oceanography*, 142, 75–90. <https://doi.org/10.1016/j.dsr2.2017.01.008>
- Berner, R.A., 1989. Biogeochemical cycles of carbon and sulfur and their effect on atmospheric oxygen over Phanerozoic time. *Palaeogeography, Palaeoclimatology, Palaeoecology*, 75, 97–122. [https://doi.org/10.1016/0031-0182\(89\)90186-7](https://doi.org/10.1016/0031-0182(89)90186-7)
- Blair, N.E. & Aller, R.C., 2012. The fate of terrestrial organic carbon in the marine environment. *Annual Review of Marine Sciences*, 4, 401–423. <https://doi.org/10.1146/annurev-marine-120709-142717>
- Blair, N.E., Leithold, E.L., Brackley, H., Trustrum, N., Page, M. & Childress, L., 2010. Terrestrial sources and export of particulate organic carbon in the Waipaoa sedimentary system: problems, progress and processes. *Marine Geology*, 270/1–4, 108–118. <https://doi.org/10.1016/j.margeo.2009.10.016>
- Bonnell, C., 2005. Mise en place des lobes distaux dans les systèmes turbiditiques actuels : Analyse comparée des systèmes du Zaïre, Var et Rhône. Unpublished Ph.D. thesis, Université de Bordeaux I, Talence, 275 p.
- Burdige, D.J., 2005. Burial of terrestrial organic matter in marine sediments; a re-assessment. *Global Biogeochemical Cycles*, 19, 4, 7 p. <https://doi.org/10.1029/2004GB002368>
- Cadée, G.C., 1984. Particulate and dissolved organic carbon and chlorophyll A in the Zaire River, estuary and plume. *Netherlands Journal of Sea Research*, 17, 426–440. [https://doi.org/10.1016/0077-7579\(84\)90059-0](https://doi.org/10.1016/0077-7579(84)90059-0)
- Canals, M., Puig, P., Durrieu de Madron, X., Heussner, S., Palanques, A. & Fabres, J., 2006. Flushing submarine canyons. *Nature*, 444, 354–357. <http://dx.doi.org/10.1038/nature05271>
- Cochoinat, P., 1993. GUINNESS 2 cruise, RV Le Suroît. <http://dx.doi.org/10.17600/93000190>
- Cochoinat, P., 1998. ZAIANGO2 cruise, RV L'Atalante. <http://dx.doi.org/10.17600/98010110>
- Cochoinat, P. & Robin, A., 1992. GUINNESS I cruise, RV L'Atalante. <http://dx.doi.org/10.17600/92004211>
- Copard, Y., Di-Giovanni, C., Martaud, T., Albéric, P. & Oliver, J.-E., 2006. Using Rock-Eval 6 pyrolysis for tracking fossil organic carbon in modern environments: implications for the roles of erosion and weathering. *Earth Surface Processes and Landforms*, 31, 135–153. <https://doi.org/10.1002/esp.1319>
- Coynel, A., Seyler, P., Etcheber, H., Meybeck, M. & Orange, D., 2005. Spatial and seasonal dynamics of total suspended sediment and organic carbon species in the Congo River. *Global Biogeochemical Cycles* 19, 4, 17 p. <https://doi.org/10.1029/2004GB002335>
- Croguennec, C., Ruffine, L., Dennielou, B., Baudin, F., Caprais, J.-C., Guyader, V., Bayon, G., Brandily, C., Le Bruchec, J., Bollinger, C., Germain, Y., Droz, L., Babonneau, N. & Rabouille, C., 2017. Evidence and age estimation of mass wasting at the distal lobe of the Congo deep-sea fan. *Deep-Sea Research II: Topical Studies in Oceanography*, 142, 50–63. <https://doi.org/10.1016/j.dsr2.2016.12.013>

- Dalibard, M., Popescu, S.M., Maley, J., Baudin, F., Melinte-Dobrescu, M.C., Pittet, B., Marsset, T., Dennielou, B., Droz, L. & Suc, J.P., 2014. High resolution vegetation history of West Africa during the last 145 ka. *Geobios*, 47/4, 183–198. <https://doi.org/10.1016/j.geobios.2014.06.002>
- Dennielou, B., 2002. Rapport Final ZaïAngo: Ages et taux d'accumulation du deep-sea fan du Zaïre, synthèse des éléments de stratigraphie. IFREMER, Brest (unpublished report).
- Dennielou, B., Droz, L., Jacq, C., Babonneau, N., Bonnel, C., Picot, M., Le Saout, M., Saout, J., Bez, M., Savoye, B., Olu, K. & Rabouille, C., 2017. Morphology, structure, composition and build-up processes of the active Congo channel-mouth lobe complex with inputs from remotely operated underwater vehicle (ROV) multibeam and video surveys. *Deep-Sea Research II: Topical Studies in Oceanography*, 142, 25–49. <https://doi.org/10.1016/j.dsr2.2017.03.010>
- Droz, L., Rigaut, F., Cochonot, P. & Tofani, R., 1996. Morphology and recent evolution of the Zaire turbidite system (Gulf of Guinea). *Geological Society of America Bulletin*, 108, 253–269. [https://doi.org/10.1130/0016-7606\(1996\)108<0253:MAREOT>2.3.CO;2](https://doi.org/10.1130/0016-7606(1996)108<0253:MAREOT>2.3.CO;2)
- Droz, L., Marsset, T., Ondreas, H., Lopez, M., Savoye, B. & Spy-Anderson, L., 2003. Architecture of an active mud-rich turbidite system: the Zaire Fan (Congo-Angola margin southeast Atlantic). Results from ZaïAngo 1 and 2 cruises. *American Association of Petroleum Geologists Bulletin*, 87/7, 1145–1168. <https://doi.org/10.1306/03070300013>
- Eisma, D. & Kalf, J., 1984. Dispersal of Zaire River suspended matter in the estuary and the Angola basin. *Netherlands Journal of Sea Research*, 17/2–4, 385–411. [https://doi.org/10.1016/0077-7579\(84\)90057-7](https://doi.org/10.1016/0077-7579(84)90057-7)
- Ferry, J.-N., Babonneau, N., Mulder, T., Parize, O. & Raillard, S., 2004. Morphogenesis of Congo submarine canyon and valley: implications about the theories of the canyons formation. *Geodinamica Acta*, 17, 241–251. <https://doi.org/10.3166/ga.17.241-251>
- Galy, V. & Eglinton, T.I., 2011. Protracted storage of biospheric carbon in the Ganges–Brahmaputra basin. *Nature Geoscience*, 4, 843–847. <https://doi.org/10.1038/ngeo1293>
- Galy, V., France-Lanord, C., Beyssac, O., Faure, P., Kudrass, H. & Plahol, F., 2007. Efficient organic carbon burial in the Bengal fan sustained by the Himalayan erosional system. *Nature*, 450, 407–411. <https://doi.org/10.1038/nature06273>
- Galy, V., Peucker-Ehrenbrink, B. & Eglinton, T., 2015. Global carbon export from the terrestrial biosphere controlled by erosion. *Nature*, 521, 204–207. <https://doi.org/10.1038/nature14400>
- Gervais, A., Mulder, T., Savoye, B., Migeon, S. & Cremer, M., 2001. Recent processes of levee formation on the Zaire deep-sea fan. *Comptes Rendus de l'Académie des Sciences (Paris)*, Earth and Planetary Sciences, 332, 371–378. [https://doi.org/10.1016/S1251-8050\(01\)01550-6](https://doi.org/10.1016/S1251-8050(01)01550-6)
- Haese, R.R., Wallmann, K., Dahmke, A., Kretzmann, U., Müller, P.J. & Schulz, H.D., 1997. Iron species determination to investigate early diagenetic reactivity in marine sediments. *Geochimica et Cosmochimica Acta*, 61/1, 63–72. [https://doi.org/10.1016/S0016-7037\(96\)00312-2](https://doi.org/10.1016/S0016-7037(96)00312-2)
- Hedges, J.I. & Keil, R.G., 1995. Sedimentary organic matter preservation: an assessment and speculative synthesis. *Marine Chemistry*, 49, 81–115. [https://doi.org/10.1016/0304-4203\(95\)00008-F](https://doi.org/10.1016/0304-4203(95)00008-F)
- Heezen, B.C., Menzies, R.J., Schneider, E.D., Ewing, W.M. & Granelli, N.C.L., 1964. Congo Submarine Canyon. *American Association of Petroleum Geologists Bulletin*, 48, 1126–1149. <https://doi.org/10.1306/BC743D7F-16BE-11D7-8645000102C1865D>
- Heussner, S., Durrieu de Madron, X., Calafat, A., Canals, M., Carbonne, J., Delsaut, N. & Saragoni, G., 2006. Spatial and temporal variability of downward particle fluxes on a continental slope: lessons from an 8-yr experiment in the Gulf of Lions (NW Mediterranean). *Marine Geology*, 234, 63–92. <https://doi.org/10.1016/j.margeo.2006.09.003>
- Hilton, R.G., Galy, A. & Hovius, N., 2008. Riverine particulate organic carbon from an active mountain belt: importance of landslides. *Global Biogeochemical Cycles*, 22/1, GB1017. <https://doi.org/10.1029/2006GB002905>
- Hsu, F.-H., Su, C.-C., Wang, C.-H., Lin, S., Liu, J. & Huh, C.-A., 2014. Accumulation of terrestrial organic carbon on an active continental margin offshore southwestern Taiwan: Source-to-sink pathways of river-borne organic particles. *Journal of Asian Earth Sciences*, 91, 163–173. <https://doi.org/10.1016/j.jseaes.2014.05.006>
- Jansen, J.H.F., van Weering, T.C.E., Gieles, R. & van Iperen, J., 1984. Middle and Late Quaternary oceanography and climatology of the Zaire-Congo fan and adjacent eastern Angola Basin. *Netherlands Journal of Sea Research*, 17/2–4, 201–249. [https://doi.org/10.1016/0077-7579\(84\)90048-6](https://doi.org/10.1016/0077-7579(84)90048-6)
- Khripounoff, A., 2003. BIOZAIRE 3 cruise, RV L'Atalante. <http://dx.doi.org/10.17600/3010120>
- Khripounoff, A., Vangriesheim, A., Babonneau, N., Crassous, P., Savoye, B. & Dennielou, B., 2003. Direct observation of intense turbidity current activity in the Zaire submarine valley at 4000 m water depth. *Marine Geology*, 194, 151–158. [https://doi.org/10.1016/S0025-3227\(02\)00677-1](https://doi.org/10.1016/S0025-3227(02)00677-1)
- Kinga-Mouzéo, M., 1986. Transport particulaire actuel du fleuve Congo et de quelques affluents : enregistrement quaternaire dans l'éventail détritique profond (sédimentologie, minéralogie et géochimie). Unpublished Ph.D. thesis, Université de Perpignan, Perpignan, 261 p.
- Kuehl, S., Alexander, C.R., Blair, N.E., Harris, C.K., Marsaglia C.M., Ogston, A.S., Orpin, A.R., Roering, J.J., Bever, A.J., Bilderback, E.L., Carter, L., Cerovski-Darriau, C., Childress, L.B., Corbett, D.R., Hale, R.P., Leithold, E.L., Litchfield, N., Moriarty, J.M., Page, M.J., Pierce, L.E.R., Upton, P. & Walsh, J.P., 2016. A source-to-sink perspective of the Waipaoa River margin. *Earth-Science Reviews*, 153, 301–334. <https://doi.org/10.1016/j.earscirev.2015.10.001>
- Laraque, A., Mahé, G., Orange, D. & Marieu, B., 2001. Spatio-temporal variations in hydrological regimes within Central Africa during the XXth century. *Journal of Hydrology*, 245/1–4, 104–117. [https://doi.org/10.1016/S0022-1694\(01\)00340-7](https://doi.org/10.1016/S0022-1694(01)00340-7)
- Leithold, E.L., Blair, N.E. & Wegmann, K., 2016. Source-to-sink sedimentary systems and global carbon burial: A river runs through it. *Earth-Science Reviews*, 153, 30–42. <https://doi.org/10.1016/j.earscirev.2015.10.011>
- Mahé, G., 1995. Modulation annuelle et fluctuations interannuelles des précipitations sur le bassin versant du Congo. In Olivry, J.C. & Boulégue, J. (eds), *Grands Bassins Fluviaux Périallantiques : Congo, Niger, Amazone*. ORSTOM, Paris, Colloques et Séminaires, 13–26.
- Marsset, T. & Droz, L., 2010. REPRESAI LEG1 cruise, RV Pourquoi pas? <http://dx.doi.org/10.17600/10030170>
- Marsset, T., Droz, L., Dennielou, B. & Pichon, E., 2009. Cycles in the architecture of the Quaternary Zaire turbidite system: a possible link with climate. In Kneller, B. (ed.), *External Controls on Deep-Water Depositional Systems*. SEPM Special Publication, 92, 89–106. <https://doi.org/10.2110/sepmsp.092.089>
- Méjanelle, L., Rivière, B., Pinturier, L., Khripounoff, K., Baudin, F. & Dachs, J., 2017. Aliphatic hydrocarbons and triterpenes of the Congo deep sea fan. *Deep-Sea Research II: Topical Studies in Oceanography*, 142, 109–124. <https://doi.org/10.1016/j.dsr2.2017.06.003>
- Migeon, S., Savoye, B., Babonneau, N. & Spy-Anderson, F.-L., 2004. Processes of sediment-wave construction along the present-day Zaire deep-sea meandering channel: role of meanders and flow stripping. *Journal Sedimentary Research*, 74/4, 580–598. <https://doi.org/10.1306/091603740580>
- Monaco, A., Biscaye, P., Soyer, J., Pocklington, R. & Heussner, S., 1990. Particle fluxes and ecosystem response on a continental margin: the 1985–1988 Mediterranean ECOMARGE experiment. *Continental Shelf Research*, 10, 809–839. [https://doi.org/10.1016/0278-4343\(90\)90061-P](https://doi.org/10.1016/0278-4343(90)90061-P)
- Mulder, T. & Etienne, S., 2010. Lobes in deep-sea turbidite systems: State of the art. *Sedimentary Geology*, 229/3, 75–80. <https://doi.org/10.1016/j.sedgeo.2010.06.011>
- Olu, K., 2011. WACS cruise, R/V Pourquoi Pas ? <http://dx.doi.org/10.17600/11030010>
- Pastor, L., Toffin, L., Decker, C., Olu, K., Cathalot, C., Lesongeur, F., Caprais, J.-C., Bessette, S., Brandily, C., Taillefert, M. & Rabouille, C., 2017. Early diagenesis in the sediments of the Congo deep-sea fan dominated by massive terrigenous deposits: Part III - Sulfate- and methane-based microbial processes. *Deep-Sea Research II: Topical Studies in Oceanography*, 142, 139–150. <https://doi.org/10.1016/j.dsr2.2017.03.011>
- Picot, M., 2015. Cycles sédimentaires dans le système turbiditique du Congo : nature et origine. Unpublished Ph.D. thesis, Université de Bretagne occidentale, Brest, 368 p.
- Picot, M., Droz, L., Marsset, T., Dennielou, B. & Bez, M., 2016. Controls on turbidite sedimentation: insights from a quantitative approach of channels and lobes architectural parameters (Late Quaternary Congo fan). *Marine and Petroleum Geology*, 72, 423–446. <https://doi.org/10.1016/j.marpetgeo.2016.02.004>
- Picot, M., Marsset, T., Droz, L., Dennielou, B., Baudin, F., Hermoso, M., de Rafelis, M., Sionneau, T., Cremer, M., Laurent, D. & Bez, M., 2019. Monsoon control on channel avulsions in the Late Quaternary Congo Fan. *Quaternary Science Reviews*, 204, 149–171. <https://doi.org/10.1016/j.quascirev.2018.11.033>
- Pozzato, L., Cathalot, C., Berrached, C., Toussaint, F., Stetten, E., Caprais, J.C., Pastor, L., Olu, K. & Rabouille, C., 2017. Early diagenesis in the Congo deep-sea fan sediments dominated by massive terrigenous deposits: Part I – Oxygen consumption and organic carbon mineralization using a micro-electrode approach. *Deep Sea Research Part II: Topical Studies in Oceanography*, 142, 125–138. <https://doi.org/10.1016/j.dsr2.2017.05.010>
- Probst, J.L., Mortatti, S. & Tardy, Y., 1994. Carbon river fluxes and weathering CO₂ consumption in the Congo and Amazon River basins. *Applied Geochemistry*, 7, 1–13. [https://doi.org/10.1016/0883-2927\(94\)90047-7](https://doi.org/10.1016/0883-2927(94)90047-7)

- Pruski, A.M., Decker, C., Stetten, E., Vétion, G., Martinez, P., Charlier, K., Senyariach, C. & Olu, K., 2017. Energy transfer in the Congo turbiditic system: from terrestrially-derived organic matter to chemosynthetic food webs. *Deep-Sea Research II: Topical Studies in Oceanography*, 142, 197–218. <https://doi.org/10.1016/j.dsr2.2017.05.011>
- Rabouille, C., 2011. CONGOLOBE cruise, R/V Pourquoi Pas ? <http://dx.doi.org/10.17600/11030170>
- Rabouille, C., Caprais, J.C., Lansard, B., Crassous, P., Dedieu, K., Reyss, J.L. & Khripounoff, A., 2009. Organic matter budget in the Southeast Atlantic continental margin close to the Congo Canyon: In situ measurements of sediment oxygen consumption. *Deep-Sea Research II: Topical Studies in Oceanography*, 56, 2223–2238. <https://doi.org/10.1016/j.dsr2.2009.04.005>
- Rabouille, C., Baudin, F., Dennielou, B. & Olu, K., 2017a. Organic carbon transfer and ecosystem functioning in the terminal lobes of the Congo deep-sea fan: outcomes of the Congolobe project. *Deep-Sea Research II: Topical Studies in Oceanography*, 142, 1–6. <https://doi.org/10.1016/j.dsr2.2017.07.006>
- Rabouille, C., Olu, K., Baudin, F., Khripounoff, A., Dennielou, B., Arnaud-Haond, S., Babonneau, N., Bayle, C., Beckler, J., Bessette, S., Bombled, B., Bourgeois, S., Brandily, C., Caprais, J.C., Cathalot, C., Charlier, K., Corvaisier, R., Croguennec, C., Cruaud, P., Decker, C., Droz, L., Gayet, N., Godfroy, A., Hourdez, S., Le Bruchec, J., Le Saout, J., Lesaout, M., Lesongeur, F., Martinez, P., Mejanelle, L., Michalopoulos, P., Mouchel, O., Noel, P., Pastor, L., Picot, M., Pignet, P., Pozzato, L., Pruski, A.M., Rabiller, M., Raimonet, M., Ragueneau, O., Reyss, J.L., Rodier, P., Ruesch, B., Ruffine, L., Savignac, F., Senyariach, C., Schnyder, J., Sen, A., Stetten, E., Sun, M.Y., Taillefert, M., Teixeira, S., Tisserat-Laborde, N., Toffin, L., Tourolle, J., Toussaint, F., Vétion, G., Jouanneau, J.M. & Bez, M., 2017b. The Congolobe project, a multidisciplinary study of Congo deep-sea fan lobe complex: Overview of methods, strategies, observations and sampling. *Deep-Sea Research II: Topical Studies in Oceanography*, 142, 7–24. <https://doi.org/10.1016/j.dsr2.2016.05.006>
- Rabouille, C., Dennielou, B., Baudin, F., Raimonet, M., Droz, L., Khripounoff, A., Martinez, P., Méjanelle, L., Michalopoulos, P., Pastor, L., Pruski, A., Ragueneau, O., Reyss, J.-L., Ruffine, L., Schnyder, J., Stetten, E., Taillefert, M., Tourolle, J. & Olu, K., 2019. Carbon and silica megasink in deep-sea sediments of the Congo terminal lobes. *Quaternary Science Reviews*, 222, <https://doi.org/10.1016/j.quascirev.2019.07.036>
- Reading, H.G. & Richards, M., 1994. Turbidite systems in deep-water basin margins classified by grain size and feeder system. *American Association of Petroleum Geologists Bulletin*, 78/5, 792–822. <https://doi.org/10.1306/A25FE3BF-171B-11D7-8645000102C1865D>
- Sanchez-Vidal, A., Canals, M., Calafat, A., Lastras, G., Pedrosa-Pamiers, R., Menendez, M., Medina, R., Company, J.B., Hereu, B., Romero, J. & Alcoverro, T., 2012. Impacts on the Deep-Sea ecosystem by a severe coastal storm. *PLoSOne*, 7/1, e30395. <http://dx.doi.org/10.1371/journal.pone.0030395>
- Savoye, B., 1998. ZAIANGO1 cruise, RV L'Atalante. <http://dx.doi.org/10.17600/98010100>
- Savoye, B. & Ondréas, H., 2000. ZAIANGOROV cruise, RV L'Atalante. <http://dx.doi.org/10.17600/10100>
- Savoye, B., Cochonat, P., Apprioual, R., Bain, O., Baltzer, A., Bellec, V., Beuzart, P., Bourillet, J., Cagna, R., Cremer, M., Crusson, A., Dennielou, B., Diebler, D., Droz, L., Ennes, J., Floch, G., Foucher, J., Guiomar, M., Harmegnies, F., Kerbrat, R., Klein, B., Khun, H., Landure, J., Lasnier, C., Le Drezen, E., Le Formal, J., Lopez, M., Loubrieu, B., Marsset, T., Migeon, S., Normand, A., Nouze, H., Ondreas, H., Pelleau, P., Saget, P., Seranne, M., Sibuet, J.C., Tofani, R. & Voisset, M., 2000. Structure et évolution récente de l'éventail turbiditique du Zaïre: Premiers résultats scientifiques des missions d'exploration ZaïAngo 1 and 2 (marge Congo-Angola). *Comptes Rendus de l'Académie des Sciences (Paris), Earth and Planetary Sciences*, 311, 211–220. [https://doi.org/10.1016/S1251-8050\(00\)01385-9](https://doi.org/10.1016/S1251-8050(00)01385-9)
- Savoye, B., Babonneau, N., Dennielou, B. & Bez, M., 2009. Geological overview of the Angola-Congo margin, the Congo deep-sea fan and its submarine valleys. *Deep-Sea Research II: Topical Studies in Oceanography*, 56, 2169–2182. <https://doi.org/10.1016/j.dsr2.2009.04.001>
- Schlünz, B. & Schneider, R.R., 2000. Transport and terrestrial organic carbon to the oceans by rivers: re-estimating flux and burial rates. *International Journal of Earth Sciences*, 88, 599–606. <https://doi.org/10.1007/s005310050290>
- Schneider, R.R., Müller, P.J. & Wefer, G., 1994. Late Quaternary paleoproductivity changes off the Congo deduced from stable carbon isotopes of planktonic foraminifera. *Palaeogeography, Palaeoclimatology, Palaeoecology*, 110/3, 255–274. [https://doi.org/10.1016/0031-0182\(94\)90087-6](https://doi.org/10.1016/0031-0182(94)90087-6)
- Schneider, R.R., Price, B., Müller, P.J., Kroon, D. & Alexander, I., 1997. Monsoon related variations in Zaire (Congo) sediment load and influence of fluvial silicate supply on marine productivity in the east equatorial Atlantic during the last 200,000 years. *Paleoceanography*, 12/3, 463–481. <https://doi.org/10.1029/96PA03640>
- Schnyder, J., Stetten, E., Baudin, F., Pruski, A.M. & Martinez, P., 2017. Palynofacies reveal fresh terrestrial organic matter inputs in the terminal lobes of the Congo deep-sea fan. *Deep-Sea Research II: Topical Studies in Oceanography*, 142, 91–108. <https://doi.org/10.1016/j.dsr2.2017.05.008>
- Seiter, K., Hensen, C., Schroter, E. & Zabel, M., 2004. Organic carbon content in surface sediments - defining regional provinces. *Deep-Sea Research Part I: Oceanographic Research Papers*, 51/12, 2001–2026. <https://doi.org/10.1016/j.dsr.2004.06.014>
- Seyler, P., Etcheber, H., Orange, D., Laraque, A., Sigha-Nkamdjou, L. & Olivry, J.C., 1995. Concentrations, fluctuations saisonnières et flux de carbone dans le bassin du Congo. In Olivry, J.C. & Boulègue, J. (eds), *Grands Bassins Fluviaux Périatlantiques : Congo, Niger, Amazone*. ORSTOM, Paris, Colloques et Séminaires, 217–228.
- Seyler, P., Coynel, A., Moreira-Turcq, P., Etcheber, H., Colas, C., Orange, D., Bricquet, J.P., Laraque, A., Guyot, J.L. & Meybeck, M., 2006. Organic carbon transported by the equatorial rivers: Example of Zaire-Congo and Amazon Rivers. In Roose, E.J., Lal, R., Feller, C., Barthes, B. & Stewart, B.A. (eds), *Soil Erosion and Carbon Dynamics*. CRC Press, Boca Raton, *Advances in Soil Science*, 255–274.
- Sibuet, M., 2001a. BIOZAIRE 1 cruise, RV L'Atalante. <http://dx.doi.org/10.17600/1010010>
- Sibuet, M., 2001b. BIOZAIRE 2 cruise, RV L'Atalante. <http://dx.doi.org/10.17600/1010130>
- Spencer, R.G.M., Hernes, P.J., Aufdenkampe, A.K., Baker, A., Gulliver, P., Stubbins, A., Aiken, G.R., Dyda, R.Y., Butler, K.D., Mwamba, V.L., Mangangu, A.M., Wabakanganzi, J.N. & Six, J., 2012. An initial investigation into the organic matter biogeochemistry of the Congo River. *Geochimica et Cosmochimica Acta*, 84, 614–627. <https://doi.org/10.1016/j.gca.2012.01.013>
- Spencer, R.G.M., Stubbins, A. & Gaillardet, J., 2014. Geochemistry of the Congo River, estuary and plume. In Bianchi, T.S., Allison, M. A. & Cai, W.J. (eds), *Biogeochemical Dynamics at Major River-Coastal Interfaces Linkages with Global Change*. Cambridge University Press, Cambridge, 3–18.
- Stetten, E., Baudin, F., Reyss, J.L., Martinez, P., Charlier, K., Schnyder, J., Rabouille, C., Dennielou, B., Coston-Guarini, J. & Pruski, A., 2015. Organic matter characterization and distribution in sediments of the terminal lobes of the Congo deep-sea fan: evidence for the direct influence of the Congo River. *Marine Geology*, 369, 182–195. <https://doi.org/10.1016/j.margeo.2015.08.020>
- Stow, D.A.V., Reading, H.G. & Collinson, J., 1996. Deep seas. In Reading, H.G. (ed.), *Sedimentary Environments: Processes, Facies and Stratigraphy*. 3rd ed. Blackwell Science, Oxford, 380–442.
- Taillefert, M., Beckler, J., Cathalot, C., Michalopoulos, P., Corvaisier, R., Kiriazis, N., Caprais, J.-C., Pastor, L. & Rabouille, C., 2017. Early diagenesis in the sediments of the Congo deep-sea fan dominated by massive terrigenous deposits: Part II – Iron-sulfur coupling. *Deep-Sea Research Part II: Topical Studies in Oceanography*, 142, 151–166. <https://doi.org/10.1016/j.dsr2.2017.06.009>
- Treignier, C., 2005. Apports en matière organique marine et terrigène sur la marge équatoriale ouest africaine : rôle joué par le canyon sous-marin du Zaïre. Approche par les biomarqueurs lipidiques. Unpublished Ph.D thesis, Université Pierre et Marie Curie, Paris, 129 p.
- Treignier, C., Derenne, S. & Saliot, A., 2006. Terrestrial and marine n-alcohol inputs and degradation processes relating to a sudden turbidity current in the Zaire canyon. *Organic Geochemistry*, 37, 1170–1184. <https://doi.org/10.1016/j.orggeochem.2006.03.010>
- van Weering, T.C.E. & van Iperen, J., 1984. Fine-grained sediments of the Zaire deep-sea fan, southern Atlantic Ocean. *Geological Society, London, Special Publications*, 15, 95–113. <https://doi.org/10.1144/GSL.SP.1984.015.01.06>
- Vangriesheim, A., Khripounoff, A. & Crassous, P., 2009. Turbidity events observed in situ along the Congo submarine channel. *Deep-Sea Research II: Topical Studies in Oceanography*, 56, 2208–2222. <https://doi.org/10.1016/j.dsr2.2009.04.004>
- Wetzel, A., 1993. The transfer of river load to deep-sea fans: a quantitative approach. *American Association of Petroleum Geologists Bulletin*, 77, 1679–1692. <https://doi.org/10.1306/BDF8EFC-1718-11D7-8645000102C1865D>